National Aeronautics and Space Administration

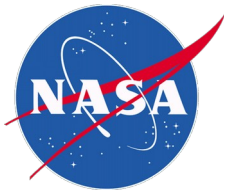

Algorithm Theoretical Basis Document (ATBD)
Version 01

NASA Measures Precipitation Fundamental Climate Data Record

Prepared for:

National Aeronautics and Space Administration (NASA)
Goddard Earth Sciences (GES) Data and Information Services Center (DISC)

Prepared by:

Chris Kidd, NASA/GSFC Code 612, Greenbelt, MD 20771, and University of Maryland, College Park, MD 20740
James Beauchamp, University of Maryland, College Park, MD 20740
Mathew Sapiano

01 June 2022

TABLE OF CONTENTS

LIST OF FIGURES

Page

LIST OF TABLES

1 INTRODUCTION

1.1 Objective

This document describes the retrieval techniques and processing sequence for the NASA Measures Precipitation Fundamental Climate Data Record. This data record exploits the observations made by passive microwave imaging radiometers between 1978 and 2020 to generate an ensemble of precipitation retrievals. The version of this ensemble described here is the initial version, (V01E) and while every effort has been made to produce an error-free product, a number of unknown issues may present in the product. Where such issues are found they will be noted and rectified in the implementation of future releases.

1.2 Revision History

Version	*Date*	*Author*	*Description*
01-00	01 July 2021	Chris Kidd, James Beauchamp & Mathew Sapiano	Initial version
01-01	01 June 2022	Chris Kidd	Minor revisions

1.3 Purpose of documentation

The purpose of this document is to describe the generation of a fundamental data record of an ensemble of precipitation products, from PMW sensors, together with a measure of their quality, at the instantaneous, footprint resolution (Level 2). This ensemble of precipitation products will provide a fundamental long-term, climate data record of precipitation spanning 43 years (1978-2020) from which changes and/or trends in precipitation may be assessed. Users will be able to take advantage of the ensemble of precipitation to assess the range of precipitation values, together with measures of their error and uncertainty, as well as using the data as a benchmark against which other precipitation data sets may be compared. Crucially, these precipitation products (at the retrieval stage) are independent of model information or other ancillary data sets therefore allowing comparisons with, or validation of, models.

1.4 Background

The measurement of precipitation is of great importance not only in its key role in linking the Earth's water and energy cycles but also because of its significant value to our society and environment, as well as being vital to all life on Earth (Skofronick-Jackson et al. 2017). In particular, the estimation of precipitation from satellite observations is essential to provide coverage across the globe due to the paucity in the representativeness of conventional observations (Kidd et al. 2017). Since the first visible and infrared satellite images were available algorithms have been developed to detect and measure precipitation. While visible/infrared images are important in monitoring our weather, more direct precipitation measurements are available through the use of passive microwave (PMW) observations. These PMW data sets extend back over 40 years to 1978 and are available through a set of Fundamental Climate Data Records (FCDRs) of PMW brightness temperatures (Tbs).

Techniques for the retrieval of precipitation have been built upon basic radiometric properties of the interaction of the precipitation-sized hydrometeors with the radiation sensed by the radiometer. More complex, physically-based precipitation retrieval schemes, as typified by the Goddard Profiling (GPROF) scheme (Kumerow et al. 2015) must use model information and ancillary data sets to better constrain the set of possible retrievals, as well as make them more computationally efficient. These retrieval techniques have to seek a compromise on providing reasonable precipitation estimates within a set of developer and user requirements. However, many techniques that rely upon simple relationships between the satellite observations and surface precipitation are nevertheless capable (Kidd et al. 1998); while not necessarily physically-based (i.e. directly reliant upon radiative transfer modeling), they do have a sound physical basis. For example, over the ocean, increases in the Tbs of the low frequency channels are strongly linked to increased rainfall, while over land, high frequency channels are linked to the precipitation-size ice in clouds. These basic criteria have been used in many techniques to make estimates of surface precipitation. Critically, for long term precipitation data records, since

these techniques are relatively simple, changes in the original satellites' observations are much easier to trace, attribute and understand than changes from more complex retrieval schemes. In particular, the use of more 'simple' techniques allow not only changes in the input data sets to be checked, but also provides a tool to be able to understand changes in more complex algorithms.

2 SATELLITE OBSERVATIONS

2.1 Satellite Sensors

The observations used in the generation of this database were acquired by the following sensors:

- Scanning Multichannel Microwave Radiometer (SMMR) onboard the Nimbus-7 satellite;
- Special Sensor Microwave/Imager (SSM/I), flown on the US Defense Meteorological Satellite Program (DMSP) F08/10/11/13/14/15 missions;
- Special Sensor Microwave Imager Sounder (SSMIS) flown on the DMSP F16/17/18/19 missions;
- TRMM Microwave Imager (TMI) flown on the Tropical Rainfall Measuring Mission (TRMM);
- GPM Microwave Imager (GMI) flown on the Global Precipitation Measurement (GPM) core observatory;
- Advanced Microwave Scanning Radiometer-E (AMSR-E) flown on the AQUA mission, and;
- Advanced Microwave Scanning Radiometer-2 (AMSR-2) flown on the Global Climate Observing Mission – Water 1 (GCOM-W1).

The characteristics of these sensors are described in more detail below.

Table 1: Passive microwave imaging radiometers commonly used for precipitation estimation; dates represent full extent of collected data.

Sensor	SMMR	SSM/I	SSMIS	AMSR	AMSR2	TMI	GMI
Satellite	Seasat Nimbus-7	DMSP-F08, F10/1/3/4/5	DMSP F16-F19	AQUA ADEOS-II	GCOMW1	TRMM	GPM
Dates	1978-1988	1987-present	2003-present	2002-2011	2012-present	1997-2015	2014-present
Orbit	Sun-sync	Sun-sync	Sun-sync	Sun-sync	Sun-sync	Non-sun sync	Non-sun sync
Scan	Conical	Conical	Conical	Conical	Conical	Conical	Conical
Frequencies (GHz)	6.6VH	-	-	6.925VH	6.925/7.3VH	-	-
	10.7VH	-	-	10.65VH	10.65VH	10.65VH	10.65VH
	18.0VH	19.35VH	19.35VH	18.70VH	18.70VH	18.70VH	18.70VH
	21.0VH	22.235V	22.235V	23.80VH	23.80VH	23.80VH	23.80V
	37.0VH	37.0VH	37.0VH	36.5VH	36.5VH	36.5VH	36.5VH
	-	-	50.3-63.3VH	-	-	-	-
	-	85.5VH	91.65VH	89.0VH	89.0VH	89.0VH	89.0VH
	-	-	150H	-	-	-	165.6VH
	-	-	183.31(2)H	-	-	-	183.31V(2)
	-	-	-	-	-	-	-

Scanning Multichannel Microwave Radiometer (SMMR)
SMMR was a conical scanning five frequency/ten channel microwave radiometer that flew on both the Seasat and Nimbus-7 satellites. The Seasat satellite was only operational for several months is 1978 (and the whereabouts of the data from the SMMR instrument on Seasat is unknown). The Nimbus-7 SMMR became operational in October 1978 and provided data until 1987. The SMMR instrument has vertical and horizontal polarization channels operating at 6.6, 10.7, 18.0, 21.0, and 37.0 GHz with resolutions vary from 120 km at 6.6 GHz to 22 km at 37 GHz. The Nimbus-7 operated in sun-synchronous polar orbit, at an altitude of

approximately 945 km and a period of 104 minutes.

The Special Sensor Microwave/Imager (SSM/I)

The SSM/I (or SSMI) was a multi-channel passive microwave radiometer that was flown on selected Defense Meteorological Satellite Program (DMSP) platforms providing data from 1987 to 2009. The DMSP operated in a sun-synchronous polar orbit with a period of about 102 minutes. The SSM/I sensor provides vertical and horizontal polarization values for 19, 37, and 85.5 GHz and vertical-only at 22 GHz. The conical scan provided scan lines spaced approximately 25 km apart at the suborbital point. The ensure contiguous measurements the 85.5 GHz channels were also collected at locations in between each scanline, allowing 12.5 km sampling. Channel resolutions vary from 12.5x15 km for the 85.5 GHz channels (oval due to the slanted viewing angle) to 60x75 km for the 19 GHz channels. The polar orbit provides nominal coverage over the latitudes 85°S-N. Further details are available in Hollinger et al. (1987, 1990).

Special Sensor Microwave Imager Sounder (SSMIS)

The SSMIS is a multi-channel passive microwave radiometer on the DMSP platforms since late 2003 and maybe considered to be a follow-on to the SSM/I instrument. The SSMIS operates in a sun-synchronous polar orbit with a period of about 102 minutes. The sensor provides vertical and horizontal polarization observations at 19, 37, and 91 GHz, vertical-only at 22 GHz and horizontal-only at 150 and 3x183 GHz. Additional channels of the SSMIS are centered around the 50-60 GHz sounding channels, but are not usually used for precipitation retrievals. The conical scanning sensor uses three separate feed horns for the 19/22 GHz, 37 GHz and 91 GHz, consequently these channels are not co-located. Resolutions range from 46.5x73.6 km for 19/22 GHz, 31.2x45.0 km for 37 GHz and 13.2x15.5 km for 91 GHz. The polar orbit provides nominal coverage over the latitudes 85°S-N.

Tropical Rainfall Measuring Mission (TRMM) Microwave Imager (TMI)

The TMI was a multi-channel passive microwave sensor onboard the TRMM satellite which operated from 1997 to 2015. TRMM operated in a low 35° inclination non-sun-synchronous orbit, with a period of 96 minutes. The sensor provided observations with vertical and horizontal polarization for 10.65, 19.35, 37.0, and 85.5 GHz and vertical only at 21.3). Resolutions vary from 37x63km at 10.65 GHz to 5x7 km at 85.5 GHz.

Global Precipitation Measurement (GPM) Microwave Imager (GMI)

The GMI is a multi-channel, conical scanning microwave radiometer operating onboard the GPM Core Observatory from 2014 to the present. The GPM satellite orbits at an altitude of 407 kilometers in a low inclination (65°) non-sun-synchronous orbit, and a period of about 92 minutes. The precession period with respect to the Sun is about 81 days, allowing the sensor to provide observation at different times of day (albeit over the precession period). The sensor provides vertical and horizontal polarization observations for the 10.65, 18.7, 36.5, 89. and 165.5 GHz frequencies and vertical-only at 23.8 and 2x 183.31 GHz. The spatial resolution varies from 18 km x 11 km (18.7 GHz) to 7 km x 4 km (89.5 GHz).

Advanced Microwave Radiometer for EOS (AMSR-E)

AMSR-E was a multi-channel, conical scanning, microwave radiometer that operated onboard the AQUA spacecraft from 2002 to 2011. The AQUA satellite was in a sun-synchronous orbit, with an inclination of 98.2°, an altitude of 705 kilometers and an orbital period of approximately 99 minutes. The sensor provides vertical and horizontal polarization observations at 6.925, 10.65, 18.7, 23.8, 36.5, and 89.0 GHz frequencies. Resolutions range from 6 x 4 km at 89 GHz through to 75 x 43 km at 6.925 GHz. The spatial sampling interval is 10 km for the 6.925 through 36.5 GHz channels and 5 km for the 89 GHz channels. Six separate feedhorns are used including two for the 89.0 GHz A-scan and B-scan.

Advanced Microwave Scanning Radiometer 2 (AMSR-2)

The AMSR-2 is a multi-channel, conical scanning, microwave radiometer onboard the Global Change Observation Mission – Water (GCOM-W1) satellite operating from 2012 to the present. The GCOM-W1 satellite operates in a sun-synchronous orbit, at an altitude of 700 km, an inclination of 98.2°, and an orbital

period of approximately 99 minutes. The sensor provides vertical and horizontal polarization measurements at 6.9, 10.7 18.7, 23.8, 36.5, and 89.0 GHz frequencies, with resolutions ranging from 5 x 3 km at 89 GHz to 35 x 62 km at 6.925 GHz. The spatial sampling is every 10 km for the 6.925 through 36.5 GHz channels and 5 km for the 89 GHz channels. Six separate feedhorns are used including two for the 89.0 GHz A-scan and B-scan.

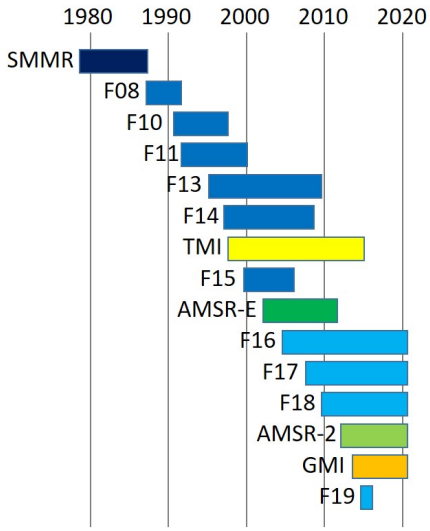

Figure 1: Timeline of the passive microwave imaging instruments used in the generated of the precipitation fundamental climate data records.

Table 2: Start and end of data record for the passive microwave instruments used in the generation of this dataset. Note that the dates relate to the availability of the data sets and consequently the precipitation retrievals, and not necessarily the operational lifetime of the satellite/sensor.

Satellite	Sensor	Start (month/year)	End (month/year)	Length of record (months)
Nimbus-7	SMMR	01/1979	08/1987	104
DMSP-F08	SSM/I	07/1987	12/1991	54
DMSP-F10	SSM/I	12/1990	11/1997	84
DMSP-F11	SSM/I	12/1991	05/2000	102
DMSP-F13	SSM/I	05/1995	11/2009	175
DMSP-F14	SSM/I	05/1997	08/2008	136
TRMM	TMI	12/1997	04/2015	209
DMSP-F15	SSM/I	02/2000	08/2006	79
AQUA	AMSR-E	06/2002	10/2011	113
DMSP-F16	SSMIS	11/2005	*12/2020*	*192*
DMSP-F17	SSMIS	03/2008	*12/2020*	*154*
DMSP-F18	SSMIS	03/2010	*12/2020*	*130*
GCOM-W1	AMSR-2	07/2012	*12/2020*	*102*
GPM	GMI	03/2014	*12/2020*	*82*
DMSP-F19	SSMIS	12/2014	02/2016	15

3 ALGORITHM DESCRIPTION

Most of the products generated in this dataset are based upon the algorithms developed for the 3rd Algorithm Intercomparison Project (AIP-3) of the Global Precipitation Climatology Project (GPCP) (Ebert, 1996), consequently all of the algorithms were developed for SSM/I measurements, but adapted here for use with other passive microwave sensors (see above).

AD1 ("Adler 1")

The AD1 or Goddard Scattering Algorithm (GSCAT) is an extension of the technique first described in Adler et al. (1993). This algorithm can be implemented over both land and water. It first uses several different SSM/I frequencies to screen out non-raining areas and then the 85 GHz (horizontal polarization) brightness temperature to estimate rain intensity that is proportional to the amount of scattering by ice and graupel aloft. The technique works best for cloud/rain processes where ice mechanisms prevail. It cannot detect rain from clouds below the freezing level. The 85 GHz brightness temperature rain rate relations are based on calculations from a combined cloud/radiative transfer model (Adler et al., 1991). The rain rate equation over water was revised based on atoll rain gauge data over the Western Pacific (Adler et al., 1994), thereby doubling rain rates over ocean regions.

Over land

if ($T_B(19V) - T_B(19H)) > 20.0$

RR = 0.0 and set the AD1 algorithm flag bit #4 (desert).

Otherwise

if ($T_B(85H) < 247.0$)

RR = $(251.0 - T_B(85H))/4.19$

Otherwise, RR = 0.0

Over water

if($T_B(85H) > T_B(37H)$ and $T_B(37H) < 185.0$)flag1=1 *! 'clear sky, cold ocean test'*

lp = $38.0 + (0.88 * T_B(19V))$ *! light precipitation test*

cs = $158.0 + (0.49 * T_B(85H))$ *! cold surface test*

if $T_B(22V) >$ lp and $T_B(22V) < 257.0$ and $T_B(22V) <$ cs) flag2=1

if (flag1 = 1 or flag2 = 1)

RR = 0.0 and set the AD1 algorithm flag bit #2 (sea ice).

Otherwise,

if ($T_B(85H) < 247.0$)

RR = $(251.0 - T_B(85H))/2.09$

Otherwise, RR = 0.0

BA0 ("Bristol Algorithm 0")

The BA0 is an ocean only method that comes from the CAL/VAL algorithm described in the DMSP Special Sensor Microwave/Imager Calibration/Validation Manual (Hollinger, 1989). First, a multichannel screening technique determines areas of rain.

calval = $-11.7939 - (0.02727 * T_B(37V) + (0.09920 * T_B(37H))$

If calval > 0, then determine RR using this equation

RR = $\exp(3.06231 - (0.0056036 * T_B(85V)) + (0.0029478 * T_B(85H)) - (0.0018119 * T_B(37V))$
$- (0.00750 * T_B(22V)) + (0.0997550 * T_B(19V))) - 8.0$

Otherwise, RR = 0.

The rain rate (RR) is then multiplied by 2.6, because CAL/VAL tends to underestimate rainfall as seen from the results of the WetNet First Precipitation Intercomparison Project (PIP-1).

BA1 ("Bristol Algorithm 1")

The BA1 or High-Frequency Vertical Frequency Difference Algorithm (HFVDFA) from Kidd and Barrett is a very simple two channel algorithm used over oceans. The physical basis for this algorithm is that the high frequency channels are more affected by the scattering from precipitation-sized particles than the lower frequency channels. Using only the 85 and 37 GHz vertically polarized channels, the rain rates (mm/hr) are determined from this equation:

$$RR = 3.55 + 0.123(T_B(37V) - T_B(85V))$$

This algorithm was calibrated against 10 months of UK Meteorological Offices FRONTIERS radar data (over the British Isles). In this calibration, only radar data within 100 km of the radar site and greater than 40 km from any coastal margins were used.

BA3 ("Bristol Algorithm 3")

The BA3 or Low-Frequency Vertical Frequency Difference Algorithm (LFVDFA) from Kidd and Barrett is a very simple two channel algorithm used over oceans. The physical basis for this algorithm is that the high frequency channels are more affected by the scattering from precipitation-sized particles than the lower frequency channels. Using only the 85 and 19 GHz vertically polarized channels, the rain rates (mm/hr) are determined from this equation:

$$RR = 6.00 + 0.110(T_B(19V) - T_B(85V))$$

This algorithm was calibrated against 10 months of UK Meteorological Offices FRONTIERS radar data (over the British Isles), as for BA1 above.

FE1 ("Ferraro 1")

The FE1 algorithm is primarily a scattering based algorithm, applicable for both land and ocean, and is a revision of the method described by Grody (1991) and presented in Ferraro et al. (1994). SSM/I measurements at both 37 and 85 GHz are depressed by Mie scattering when ice particles grow in size to approximately 0.8 mm (for 37 GHz) and 0.3 mm (for 85 GHz). Thus the 85 GHz channel is more sensitive to smaller ice particles. Grody (1991) developed a "scattering index", which is a measure of TB depression at 85 GHz due to ice particles. For FE1, separate indices, SIL and SIW, are first determined for land and water respectively. Both land and ocean algorithms were calibrated with radar data from Japan, United Kingdom, and the United States (Ferraro and Marks, 1995). It was found that that SIL/SIW values of at least 10 K were a good indicator for rain. For the ocean model, if the scattering index is not met, rain may still be present. In many mid- and high-latitude rain events or tropical warm rain, the ice scattering rain signature may be missing. For these cases, an emission based algorithm which uses estimates of atmospheric liquid water, Q19 and Q37, based on the 19 and 37 GHz channels respectively. If either of the liquid water values exceed certain thresholds, rain may be present and a rain rate can be determined. Over ocean, raining FOVs are screened for possible sea-ice and over land they are separately screened for snow, desert, and semi-arid land surfaces. Rain rates from both land and ocean algorithms are capped at 35 mm/hr.

Over land,

$SIL = 438.5 - 0.46*T_B(19V) - 1.735*T_B(22V) + 0.00589*T_B(22V)^2 - T_B(85V)$

If SIL > 10.0

$RR = 0.00513*SIL^{1.9468}$

Otherwise, set RR = 0.0

Snow screening

$TS = 175.\ K + (0.49 * T_B(85V))$

If ($T_B(22V) < 264$ K and $T_B(22V) < TS$

Set RR = 0.0 and set the FE1 algorithm flag bit #3 (snow).

Desert screening

$PD19 = T_B(19V) - T_B(19H)$

If (pd19 > 20)

Set RR = 0.0 and set the FE1 algorithm flag bit $4 (desert).

Semi-arid screening

If ($T_B(85V) > 253$ K and pd19 > 7 K)

Set RR = 0.0 and set the FE1 algorithm flag bit #4 (desert).

Over ocean,

$SIW = -174.4 + 0.715*T_B(19V) + 2.439*T_B(22V) - 0.00504*T_B(22V)2 - T_B(85V)$

If SIW > 10.0

$RR = 0.00115*SIW^{2.16832}$

Otherwise, check for an emission component.

If TB(19V) < 285 K and TB(22V) < 285 K

Q19 = -2.70 * ln(290 –TB(190)) -2.84 – 0.40 * ln(290-TB(22V))

If Q19 > 0.60, $RR = 0.001707 * (Q19*100)^{1.7359}$

Otherwise

If $T_B(37V) < 285$ K and $T_B(22V) < 285$ K

$Q37 = -1.15 * \ln(290 - T_B(37V)) - 2.99 - 0.32 * \ln(290 - T_B(22V))$

If Q37 > 0.20, $RR = 0.001707 * (Q37*100)^{1.7359}$

Otherwise, set RR=0.0

Sea-ice screening (done poleward of 45°)

$TT = 44. + 0.85 * T_B(19V)$

If (($T_B(22V) <= TT$) or If (($T_B(22V) > 264$ and $(T_B(22V) - T_B(19V)) < 2$))

Set RR = 0.0 and set the FE1 algorithm flag bit #2 (sea ice).

FE2 ("Ferraro 2")

The FE2 algorithm is an emission based algorithm used over the ocean. SSM/I window channels are capable of retrieving atmospheric liquid water (Q) over the ocean. The 19 and 37 GHz channels are especially well suited for this because they are less sensitive to scattering. For these two frequencies, variations in brightness temperature can be primarily attributed to clouds and rain. Using the vertical polarization measurements of these channels minimizes the small variations due to wind over the ocean surface and the effect of water vapor can be removed by using the 22 GHz channel. Thus atmospheric liquid water (Q19) from the 19V GHz channel or Q37 from the 37V GHz can be determined. The FE2 method uses Q19 to obtain rates. Based on examination of several global data sets, it was determined that rain is present if Q19 > 0.4 mm. Both the FE2 and FE3 algorithms were calibrated against co-incident observations of SSM/I measurements and ground based radar over the ocean from Japan, United Kingdom, and the United States (Ferraro and Marks, 1995). This algorithm uses the sea-ice screening technique used in FE1 and also rain rates were capped at 35 mm/hr.

$Q19 = -6.723 * (\ln(290 - T_B(19V)) - 2.85 - 0.405 * \ln(290 - T_B(22V)))$

If (Q19 > 0.4)

$RR = 0.6227 * \exp(Q19 * 0.8)$

Otherwise, RR = 0.0

Sea-ice screening (done poleward of 45°)

$TT = 44. + 0.85 * T_B(19V)$

If (($T_B(22V) <= TT$) or If (($T_B22V) > 264.$ and $(T_B(22V) - T_B(19V)) < 2$))

Set RR=0.0 and set the FE2 algorithm flag bit #2 (sea ice).

FE3 ("Ferraro 3")

The FE3 is an ocean only algorithm similar to the FE2, except that it uses the 37V GHz channel to determine Q37, from which a rain rate can be estimated. In determining Q37, there is a correction term, SK or SI37, to take into account the presence of scattering. A rain threshold of Q37 = 0.3 mm is used for FE3. Similar to FE1, FE2, and FE4, there is sea-ice screening and rain rates are capped at 35 mm/hr.

$SK = 62.18 + 0.773 * T_B(19V) - T_B(37V)$ for SK > 5, otherwise SK = 0.0

$Q37 = -1.679 * (\ln(290) - T_B37V - SK) - 3.01 - 0.321 * \ln(290 - T_B(22V)))$

If (Q37 > 0.3)

$RR = -0.17 + (0.3141 * Q37) + (5.501 * Q37^2)$

Otherwise, RR =0.0

Sea-ice screening (done poleward of 45°)

$TT = 44. + 0.85 * T_B(19V)$

If (($T_B(22V) <= TT$) or if (($T_B22V) > 264.$ and $(T_B(22V) - T_B(19V)) < 2$))

Set RR = 0.0 and set the FE3 algorithm flag bit #2 (sea ice).

FE4 ("Ferraro 4")

The FE4 algorithm is very similar to FE1 except some of the constant values are different.

Over land,

SIL = 451.9 – 0.44*T_B(19V) – 1.775*T_B(22V) + 0.00575*$T_B(22V)^2$ – T_B(85V)

If SIL > 10.

RR = $0.00513*SIL^{1.9468}$

Otherwise, set RR = 0.0

Snow screening

TS = 175. K + (0.49 * T_B(85V))

If (T_B(22V) < 264 K and T_B(22V) < TS

Set RR = 0.0 and set the FE4 algorithm flag bit #3 (snow).

Desert screening

PD19 = T_B(19V) – T_B(19H)

If (pd19 > 20)

Set RR = 0. and set the FE4 algorithm flag bit #4 (desert).

Semi-arid screening

If (T_B(85V) > 253 K and pd19 > 7)

Set RR = 0.0 and set the FE4 algorithm flag bit #4 (desert).

Over ocean,

SIW = -174.4 + 0.720*T_B(19V) + 2.439*T_B(22V) – 0.00504*T_B(22V)2 –T_B(85V)

If SIW > 10.

RR = $0.00115*SIW^{2.16832}$

Otherwise, check for an emission component.

If TB(19V) < 285 K and TB(22V) < 285 K

Q19 = -2.70 * ln(290 –TB(190)) -2.84 – 0.40 * ln(290-TB(22V))

If Q19 > 0.60, RR = $0.001707 * (Q19*100)^{1.7359}$

Otherwise

If T_B(37V) < 285 K and T_B(22V) < 285 K

Q37 = -1.15 * ln(290 – T_B(37V)) – 2.99 - 0.32 * ln(290 – T_B(22V))

If Q37 > 0.20, RR = $0.001707 * (Q37*100)^{1.7359}$

Otherwise, set RR=0.0

Sea-ice screening (done poleward of 45°)

TT = 44. + 0.85 * T_B(19V)

If ((T_B(22V) <= TT) or If ((T_B(22V) > 264 and (T_B(22V) – T_B(19V)) < 2))

Set RR = 0.0 and set the FE4 algorithm flag bit #2 (sea ice).

FR1 (“Ferriday 1”)

The FR1 is a physically based algorithm using its sensitivity to both emission and scattering to estimate rainfall (Ferriday and Avery, 1994). It is derived from radiative transfer calculations through an atmospheric cloud model specifying the vertical distributions of ice and liquid hydrometeors as a function of rain rate. Before the rain rate can be estimated, a screening process differentiates between non-raining background conditions and the emission/scattering from hydrometeors. Temperature and polarization difference thresholds are used to determine the presence of rain and then a linear function, fit to a linear combination of channels estimates the rain rate. There are separate screening and rain rate procedures for land and ocean and the algorithm is only applicable between 60°S to 60°N.

Over land,

Where X = -15.6 + abs((latitude + season offset)/5)

And season offset is 20 for Dec., Jan., and Feb.; -20 for June, July, and Aug.; 0 for the other months

If (T_B(37V) – T_B(37H)) < 10 and (T_B(19v) – T_B(19H)) < 10 and T_B(19v) > 255 K)

RR = (T_B(19H) + 2 * TB(85H) + X)/9.1

Otherwise,

If (T_B(37V) – T_B(37H) => 10 or (T_B(19V) – T_B(19H)) => 10, set the FR1 algorithm flag bit #4 (desert).

If (T_B(19V) < 255 K) set the FR1 algorithm flag bit #3 (snow).

RR = 0.0

Over ocean,

If (T_B(19V) – T_B(19H)) < 60 K

RR = (T_B(19H) + T_B(19V) + T_B(37H) - T_B(22V) – T_B(37V) – T_B(85H) + 170.2)/18.3

Otherwise, RR = 0 and set the FR1 algorithm flag bit #2 (sea ice).

FR2 ("Ferriday 2")

The FR2 algorithm (also from James Ferriday) was originally developed for estimating global rainfall over both land and ocean and used with F10 SSM/I data for AIP-2. Initial screening is necessary to detect rainfall and eliminate false rain signals due to ice, snow, and desert which can have brightness temperatures similar to a raining atmosphere (Fiore and Grody, 1990). Both land and ocean algorithms are based on radiative transfer calculations of upwelling radiances through an atmospheric and raining cloud model at SSM/I frequencies. Both algorithms are sensitive to both emission and scattering. Underestimation effects due to beam filling are reduced because the relationship between brightness temperature and rain rate is nearly linear.

Over land,

If (T_B(19V) > 250 K and (T_B(37V) – T_B(37H)) < 7 K and T_B(19v) – T_B(85V)) > 20 K

RR = (T_B(19V) + T_B(22V) – T_B(37V) – T_B(85V))/7.0

Otherwise,

If (T_B(37V)–T_B(37H) => 7 K or (T_B(19V) – T_B(85V)) <= 20 K, set the FR2 algorithm flag bit #4 (desert).

If(T_B(19V) <= 250 K), set the FR2 algorithm flag bit #3 (snow).

Over ocean,

If TB(19v) > 230.0

RR = (TB(19V) + TB(37V) – TB(85V) – TB(85H) + 50.0)/10.0

Otherwise RR = 0.0 and set the FR2 algorithm flag bit #2 (sea ice).

IO1 ("Iowa Algorithm 1")

The IO1 algorithm was developed at the University of Iowa (Haferman et al., 1996). In its derivation it uses a 3D radiative transfer algorithm and physical-stochastic cloud model to obtain relationships between surface rain rate and upwelling microwave brightness temperature. Although formulations were developed for both over land and water surfaces, for our work we only used the technique over water surfaces.

If TB(19H) > 219.0

RR = ln(TB(22V) – TB(19H)/62.4)/-0.199

If (TB(19H) > 176.0 and TB(19H) < 219.0

RR = ln(TB(22V) – TB(19H)/74.5)/-0.038

If TB(19H) < 176.0

RR = 0.0

NR1 ("Naval Research 1")

The NR1 algorithm (or CAL/VAL algorithm) was originally developed for the Naval Research Laboratories as a response to the Calibration/Validation efforts for all pre-launch geophysical retrieval algorithms of the DMSP F08 SSM/I. For the details of how the algorithm was developed, see Hollinger (1991). A follow on algorithm, NR2, is similar but does require the high resolution, 85 GHz channels. This algorithm has both land and ocean components; coastal areas are excluded. Data from the radars at Darwin and Kwajalein were used to develop the algorithm. The Hughes negative polarization test is first used to screen for bad data.

If (T_B(85V) – T_B(85H)) < -2.0 or (T_B(37V) – T_B(37H)) < -2.0 or (T_B(19V) – T_B(19H)) < -2.0

then set the value as indeterminate and set the algorithm flag bit #5.

Over land the following filter was used:

If(T_B(22V) – T_B(19V) <= 4 K and

(T_B(19V) + T_B(37V))/2 – (T_B(19H) + T_B(37H))/2 <= 4 K and

$T_B(85V) - T_B(37V) < 0$ K and
$T_B(19V) > 262$ K
Or
$T_B(22V) - T_B(19V) <= 4$ K and
$(T_B(19V) + T_B(37V)/2 - (T_B(19H) + T_B(37H)/2 > 4$ K and
$T_B(37V) - T_B(19V) < -3$ K and
$T_B(85V) - T_B(37V) < -5$ K and
$T_B(85H) - T_B(37H) < -4$ K and
$T_B(19V) > 257$ K, then compute rain rate
Otherwise RR = 0 and set the NR1 algorithm flag bit #4 (desert).

Over ocean:
if $(-11.7939 - (0.2727 * T_B(37V)) + (0.09920 * T_B(37H)) > 0$ then compute rain rate

The rain rate is computed with the following equations:
Over land,
$RR = \exp(3.29716 - (0.01290 * T_B(85V)) + (0.00877 * TB(85_H))) 8.0$
Over ocean,
$RR = \exp(3.06231 - (0.0056036 * T_B(85V)) + (0.0029478 * T_B(85H) - (0.0018119 * T_B(37V)))$
$- (0.00750 * TB(22V)) + (0.0997550 * TB(19V))) - 8.0$

NR2 ("Naval Research 2")
The NR2 algorithm is similar to the NR1 except that the high resolution channels at 85 GHz are only used for the land filter and not for the actual estimation of rain rate. As in the NR1 method, the Hughes negative polarization test is applied.

If $(T_B(37V) - T_B(37H)) < -2$ or $(T_B(19V) - T_B(19H)) < -2$
then set the value as indeterminate and set the algorithm flag bit #5.

Over land the following filter was used:
If$(T_B(22V) - T_B(19V) <= 4$ K and
$(T_B(19V) + T_B(37V))/2 - (T_B(19H) + T_B(37H))/2 <= 4$ K and
$T_B(85V) - T_B(37V) < 0$ K and
$T_B(19V) > 262$ K
Or
$T_B(22V) - T_B(19V) <= 4$ K and
$(T_B(19V) + T_B(37V)/2 - (T_B(19H) + T_B(37H)/2 > 4$ K and
$T_B(37V) - T_B(19V) < -3$ K and
$T_B(85V) - T_B(37V) < -5$ K and
$T_B(85H) - T_B(37H) < -4$ K and
$T_B(19V) > 257$ K, then compute rain rate
Otherwise RR = 0.0 and set the NR2 algorithm flag bit #4 (desert).

Over ocean:
If $(-11.7939 - (0.2727 * T_B(37V)) + (0.09920 * T_B(37H)) > 0$ K then compute the rain rate.

And finally the rain rate is computed with the following equations:
Over land,
$RR= \exp(-17.76849 - (0.09612 * T_B(37V)) + (0.15678*T_B(V19))) - 1.0$
Over ocean,
$RR = \exp(5.10196 - (0.05378 * T_B(37V)) + ((0.02766 * T_B(37V)) + (0.01373 * T_B(19V))) - 2.0$

PR1 ("Prabhakara 1")

The PR1 (ocean only) algorithm from Prabhakara uses the assumption that any SSM/I footprint has a log-normal distribution of brightness temperatures when rain is present. Using radiative transfer theory, the brightness temperature and polarization differences for channel 19, 37, and 85 GHz are related to the average rain rate in the footprint. The relationship adopted for the PIP-3 study was:

C = -5.0
If (T_B(37H) > 180.0 K then
RR = C * (T_B(85H) – T_B(37H))/(275.0-T_B19H))
Otherwise, RR = 0.0

SC2 ("Schlussel 2")

The SC2 algorithm (Bauer and Schlussel 1993) is based upon many radiative transfer simulations of highly variable cloud and rain situations. Multilinear regression statistics applied to simulated data are used to derive the retrieval techniques. The regressions are applied to the logarithm of the rain rates in order to spread the range for low rain amounts. Rain rates less 0.3 mm/hr are set to zero because of the difficulty in discriminating light rainfall from non-raining cloud water in the radiometric signal. This algorithm is applied only over oceans.

$$\text{Log}_{10}(RR) = 14.66 - 0.7488e{+}10/(T_B(19V))^4 - (0.04503 * T_B(22V)) + 0.5064e{+}05/(T_B(19H))^2 - 0.599e{+}05/(T_B(37H)^2 + 0.1172e{-}03 * (T_B(37V) - T_B(19H))^2$$

If RR < 0.3, set RR = 0.0

4 DATA PROCESSING

4.1 Input data

The primary source of the satellite observations was from the NASA Precipitation Processing System (PPS). The PPS ingests and processes passive microwave brightness temperatures from multiple sources and generates a consistently-calibrated Level 1 'C' (for 'calibrated') data set. While other FCDR brightness temperature records exist, inconsistencies were found between the PPS data and these other FCDR data sets, while a new FCDR data set (Fenning et al. 2021) was not available to be exploited by this project. The only non-PPS data set was that for SMMR which was sourced from the National Snow and Ice Data Center (NSIDC), available in HDF format. It should be noted however that the SMMR data has not undergone the same rigorous calibration processing that the other sensors have been subjected to. The data record (as noted above) spans from 1979 through to the end of 2020, and reflect the availability of the data on the PPS system. However, it should be noted that the PPS does not necessarily process all the data that a particularly provides, particularly where that data falls outside the quality-control boundaries (e.g. the DMSP-F15 after the implementation of the RADCOM beacon).

The PPS Level 1C brightness temperatures (all sensors except SMMR) can be obtained from:
https://gpm.nasa.gov/data
While the SMMR Level 1B brightness temperature data can be obtained from:
https://nsidc.org/data/NSIDC-0036/versions/1

4.2 Brightness Temperature Adjustments

The precipitation retrieval algorithms described above have been developed using SSM/I microwave brightness temperatures. The retrievals here use different sensors with different channel characteristics, such as frequency and resolution (see Table 3 and 4). Although the PPS Level 1C data are 'consistently calibrated', that does not necessarily mean that they are inter-calibrated, consequently adjustments are required to ensure that the brightness temperatures observed by one sensor and similar to those observed by another sensor. A simple adjustment scheme was adopted whereby the mean of the monthly mean brightness temperatures of each channel of each sensor was compared against that of the mean of each channel for all of the SSM/I sensors.

This was done for land and sea for 30°N-30°S (to avoid any snow/ice issues). The differences between each sensor and the mean of the SSM/I provided offsets that were applied before applying the retrieval algorithm. While not perfect, the adjustments reflected the overall background bias between the different sensors and allow the algorithms to be consistently applied. The mean brightness temperatures of each of the channels is shown in Table 3 below for sea and land, followed by Table 4 which shows the offsets applied to each channel and each sensor. Note however that the differences between the individual SSM/I sensors were not corrected for since these were mainly less than 1.0K and would likely reflect the differences in overpass time.

The tables include the frequency of observation for each channel/sensor: it should be noted that there are differences between the sensors within the channel groups, e.g. 18.0 GHz vs 18.7 GHz vs 19.35 GHz, etc. These differences will produce slightly different observed brightness temperatures dependent upon geophysical properties and atmospheric contributions. The lower table of the channel offsets highlights (in bold) the differences of 1.0K or greater. It can be noted that the SMMR in particular has significant offsets, in part since it has not been rigorously calibrated as have the other instruments. Other large offsets, such as the GMI over the ocean, are likely to be due to differences in the Earth Incidence Angle that affects the polarization of the observation, which are most noticeable over the oceans and water surfaces.

Table 3: Mean brightness temperatures by sensor and channel for (top) sea, and (bottom) land.

S	Nimbus-7 SMMR	AQUA AMSRE	GCOM AMSR2	F08 SSMI	F10 SSMI	F11 SSMI	F13 SSMI	F14 SSMI	F15 SSMI	F16 SSMIS	F17 SSMIS	F18 SSMIS	F19 SSMIS	TRMM TMI	GPM GMI
	18.0	*18.7*	*18.7*	*19.35*	*19.35*	*19.35*	*19.35*	*19.35*	*19.35*	*19.35*	*19.35*	*19.35*	*19.35*	*18.7*	*18.7*
V	190.8	205.6	206.1	206.4	205.7	206.7	206.0	206.3	205.8	209.2	207.9	208.8	208.2	206.7	200.3
H	129.4	140.4	137.5	146.2	146.2	146.8	147.2	147.3	147.4	148.4	148.5	148.3	148.9	146.3	138.0
	21.0	*23.8*	*23.8*	*22.235*	*22.235*	*22.235*	*22.235*	*22.235*	*22.235*	*22.235*	*22.235*	*22.235*	*22.235*	*23.8*	*23.8*
V	219.2	237.5	238.9	238.7	238.1	239.8	239.1	239.4	239.1	241.2	240.3	241.0	241.2	231.3	233.9
	37.0	*36.5*	*36.5*	*37.0*	*37.0*	*37.0*	*37.0*	*37.0*	*37.0*	*37.0*	*37.0*	*37.0*	*37.0*	*36.5*	*36.5*
V	219.0	226.1	226.6	223.0	222.3	223.0	222.3	222.6	222.1	223.5	223.6	224.2	224.4	223.0	222.0
H	165.2	167.8	167.4	166.4	166.2	166.6	167.1	167.1	167.0	167.8	167.8	167.7	168.5	166.4	167.0
	-	*89.0*	*89.0*	*85.5*	*85.5*	*85.5*	*85.5*	*85.5*	*85.5*	*91.65*	*91.65*	*91.65*	*91.65*	*89.0*	*89.0*
V	-	267.0	271.8	267.6	267.4	268.3	268.1	268.3	268.1	271.6	271.3	271.7	271.6	268.0	270.0
H	-	244.8	249.5	242.7	242.7	244.6	244.6	244.7	244.8	251.3	250.7	250.9	251.2	243.7	248.3

L	Nimbus-7 SMMR	AQUA AMSRE	GCOM AMSR2	F08 SSMI	F10 SSMI	F11 SSMI	F13 SSMI	F14 SSMI	F15 SSMI	F16 SSMIS	F17 SSMIS	F18 SSMIS	F19 SSMIS	TRMM TMI	GPM GMI
	18.0	*18.7*	*18.7*	*19.35*	*19.35*	*19.35*	*19.35*	*19.35*	*19.35*	*19.35*	*19.35*	*19.35*	*19.35*	*18.7*	*18.7*
V	275.8	283.8	286.4	282.6	285.2	283.3	283.0	284.0	284.9	284.2	283.6	284.1	283.7	284.8	285.0
H	262.4	270.1	273.3	269.7	272.5	271.1	271.2	272.1	273.1	271.3	270.9	271.5	271.6	271.7	272.4
	21.0	*23.8*	*23.8*	*22.235*	*22.235*	*22.235*	*22.235*	*22.235*	*22.235*	*22.235*	*22.235*	*22.235*	*22.235*	*23.8*	*23.8*
V	274.7	285.1	286.8	281.8	283.7	283.5	283.2	283.9	284.9	284.1	283.6	284.0	284.2	284.9	285.7
	37.0	*36.5*	*36.5*	*37.0*	*37.0*	*37.0*	*37.0*	*37.0*	*37.0*	*37.0*	*37.0*	*37.0*	*37.0*	*36.5*	*36.5*
V	276.2	284.9	285.4	281.1	284.9	281.7	281.4	282.5	283.6	282.2	282.0	282.4	281.6	283.2	283.8
H	265.8	274.7	275.5	270.9	274.8	272.2	272.2	273.2	274.3	272.9	272.3	272.7	272.3	273.3	274.4
	-	*89.0*	*89.0*	*85.5*	*85.5*	*85.5*	*85.5*	*85.5*	*85.5*	*91.65*	*91.65*	*91.65*	*91.65*	*89.0*	*89.0*
V	-	284.0	284.9	280.1	282.6	281.0	281.0	281.9	283.0	282.2	281.6	282.2	281.5	282.7	283.5
H	-	278.7	279.8	272.8	276.3	275.8	275.9	276.4	277.8	277.9	276.9	277.4	276.9	277.3	278.7

Table 4: Brightness temperatures differences (sensor minus mean SSM/I) by sensor and channel for (top) sea, and (bottom) land. Bold figures indicate differences > 1.0K.

S	Nimbus-7 SMMR	AQUA AMSRE	GCOM AMSR2	F08 SSMI	F10 SSMI	F11 SSMI	F13 SSMI	F14 SSMI	F15 SSMI	F16 SSMIS	F17 SSMIS	F18 SSMIS	F19 SSMIS	TRMM TMI	GPM GMI
	18.0	*18.7*	*18.7*	*19.35*	*19.35*	*19.35*	*19.35*	*19.35*	*19.35*	*19.35*	*19.35*	*19.35*	*19.35*	*18.7*	*18.7*
V	**-15.4**	-0.6	-0.1	0.2	-0.5	0.5	-0.2	0.1	-0.4	**3.0**	**1.7**	**2.6**	**2.0**	0.5	**-5.9**
H	**-17.4**	**-6.4**	-9.3	-0.6	-0.6	0.0	0.4	0.5	0.6	**1.6**	**1.7**	**1.5**	**2.1**	-0.5	**-8.8**
	21.0	*23.8*	*23.8*	*22.235*	*22.235*	*22.235*	*22.235*	*22.235*	*22.235*	*22.235*	*22.235*	*22.235*	*22.235*	*23.8*	*23.8*
V	**-19.8**	**-1.5**	-0.1	-0.3	-0.9	0.8	0.1	0.4	0.1	**2.2**	**1.3**	**2.0**	**2.2**	**-7.7**	**-5.1**
	37.0	*36.5*	*36.5*	*37.0*	*37.0*	*37.0*	*37.0*	*37.0*	*37.0*	*37.0*	*37.0*	*37.0*	*37.0*	*36.5*	*36.5*
V	**-3.5**	**3.6**	**4.1**	0.5	-0.2	0.5	-0.2	0.1	-0.4	**1.0**	**1.1**	**1.7**	**1.9**	0.5	-0.5
H	**-1.5**	**1.1**	0.7	-0.3	-0.5	-0.1	0.4	0.4	0.3	**1.1**	**1.1**	**1.0**	**1.8**	-0.3	0.3
	-	*89.0*	*89.0*	*85.5*	*85.5*	*85.5*	*85.5*	*85.5*	*85.5*	*91.65*	*91.65*	*91.65*	*91.65*	*89.0*	*89.0*
V	-	**-1.0**	**3.8**	-0.4	-0.6	0.3	0.1	0.3	0.1	**3.6**	**3.3**	**3.7**	**3.6**	0.0	**2.0**
H	-	0.8	**5.5**	**-1.3**	**-1.3**	0.6	0.6	0.7	0.8	**7.3**	**6.7**	**6.9**	**7.2**	-0.3	**4.3**

L	Nimbus-7 SMMR	AQUA AMSRE	GCOM AMSR2	F08 SSMI	F10 SSMI	F11 SSMI	F13 SSMI	F14 SSMI	F15 SSMI	F16 SSMIS	F17 SSMIS	F18 SSMIS	F19 SSMIS	TRMM TMI	GPM GMI
	18.0	*18.7*	*18.7*	*19.35*	*19.35*	*19.35*	*19.35*	*19.35*	*19.35*	*19.35*	*19.35*	*19.35*	*19.35*	*18.7*	*18.7*
V	**-8.0**	0.0	**2.6**	**-1.2**	**1.4**	-0.5	-0.8	0.2	**1.1**	0.4	-0.2	0.3	-0.1	**1.0**	**1.2**
H	**-9.2**	**-1.5**	**1.7**	**-1.9**	0.9	-0.5	-0.4	0.5	**1.5**	-0.3	-0.7	-0.1	0.0	0.1	0.8
	21.0	*23.8*	*23.8*	*22.235*	*22.235*	*22.235*	*22.235*	*22.235*	*22.235*	*22.235*	*22.235*	*22.235*	*22.235*	*23.8*	*23.8*
V	**-8.8**	**1.6**	**3.3**	**-1.7**	0.2	0.0	-0.3	0.4	**1.4**	0.6	0.1	0.5	0.7	**1.4**	**2.2**
	37.0	*36.5*	*36.5*	*37.0*	*37.0*	*37.0*	*37.0*	*37.0*	*37.0*	*37.0*	*37.0*	*37.0*	*37.0*	*36.5*	*36.5*
V	**-6.3**	**2.4**	**2.9**	**-1.4**	**2.4**	-0.8	**-1.1**	0.0	**1.1**	-0.3	-0.5	-0.1	-0.9	0.7	**1.3**
H	**-7.1**	**1.8**	**2.6**	**-2.0**	**1.9**	-0.7	-0.7	0.3	**1.4**	0.0	-0.6	-0.2	-0.6	0.4	**1.5**
	-	*89.0*	*89.0*	*85.5*	*85.5*	*85.5*	*85.5*	*85.5*	*85.5*	*91.65*	*91.65*	*91.65*	*91.65*	*89.0*	*89.0*
V	-	**2.4**	**3.3**	**-1.5**	**1.0**	-0.6	-0.6	0.3	**1.4**	0.6	0.0	0.6	-0.1	**1.1**	**1.9**
H	-	**2.9**	**4.0**	**-3.0**	0.5	0.0	0.1	0.6	**2.0**	**2.1**	**1.1**	**1.6**	**1.1**	**1.5**	**2.9**

4.3 Geolocation

The majority of the retrieval techniques used in the generation of the precipitation products described here use multi-channel observations. While these multi-channel observations would ideally observe the same area and location on the Earth's surface, physical and engineering aspects means that the observations may not align perfectly. In particular, different frequencies result in different spatial resolutions, while the placement of the feedhorns for different channels on the sensor result in different center location for the fields-of-view. While differences in the latter are kept generally small, towards the edge of swath in particular, the scan position cannot necessarily be relied upon to provide co-located observations. Many retrieval schemes take advantage of the fact that the lower frequency channels have poorer spatial resolutions and thus the high frequency channels with greater spatial sampling will always be within the footprint of the low frequency channel for the same scan position. However, the precipitation retrievals generated here use co-located footprints to ensure that the observed brightness temperatures are aligned as much as is practically possible.

The **SMMR instrument** scan geometry is somewhat unique and although it is technically a conically-scanning instrument, the actual scan is back-and-forth. Since the whole scanning system has to stop at the edge of each scan (at the swath edges), the scanning mechanism has to slow down before reversing, thus the sampling across the scan increases towards the edge of scan/swath. Furthermore, a 'switch' determined the polarization of the measurements, the horizontal polarized observations being gathered on the outward portion of the scan, and the vertically polarized observations being gathered on the return portion. Therefore, since the vertical and horizontal polarization observations are gathered separately the horizontal and vertical channels are not co-located.

Data for the other sensors used here are provided by the NASA PPS and have the geolocation information organized in groups (S1-6), with each group relating to channels with the same geolocation. Each group also

has its own time variables (year, month, day, hour, minute, and second) and quality flags associated with it. Except for GMI, the high frequency channels are sampled at least twice as much as that for the other channels, primarily to ensure contiguous (gap-free) coverage of the observations. The products generated here use the high-frequency channel geolocation information. Where a particular retrieval scheme only uses the lower frequencies (and fewer samples) the high-frequency geolocation information is still used, but where a retrieval has been made with no corresponding low-frequency observation the algorithm flag has been set (see below).

The **SSM/I** 19, 22 and 37 GHz channels are in the S1 group with the same geolocation. For each orbit, there are *nscan* scans x 64 scan positions (the number of scans per orbit varies). The two high resolution channels at 85 GHz are in the S2 group and have 2x *nscan* x 128 scan positions. Retrievals are generated at the S2 geolocations, with the closest corresponding S1 geolocation observations. In the case of the SSM/I, where the 19, 22, and 37 GHz channels share the same latitude/longitudes, it will be the same geolocation for all five low frequency channels. Certain algorithms (FE2, FE3, IO1, NR2, and SC2) do not use the high resolution channels although retrievals are still generated at the high resolution geolocations.

The **SSMIS** 19.35 and 22.235 GHz channels are in group S1 with *nscans* x 90 scan positions. The 37 GHz channels are in S2 also with *nscans* x 90 scan positions, while the two high resolution channels, at 91.665 GHz have *nscans* x 180 scan positions. The rain rates are determined at the location of the high resolution channels and the nearest footprint for the S1 and S2 channels are determined separately.

The **TMI** 19.35 21.3 and 37.0 GHz are grouped in S2 with dimension of *nscans* x 104 scan positions (the 10.65 GHz channels are in group S1, but are not used here). The two high resolution channels (85 GHz) are in group S3 with *nscans* x 208 scan positions. The nearest geolocation of the S2 group is matched with each high resolution channel footprint.

The **GMI** Level 1C-R data is used. This has already been processed to ensure that all channels are geolocated with *nscans* x 221 scan positions (no further geolocation processing is required).

The **AMSRE** geolocation is split into six groups: 10.65 GHz in S1, 18.7 GHz in S2, 23.8 GHz in S3, 37 GHz in S4, while the 89 GHz A-scan is in S5 and the 89.0 GHz B-scan is in S6. Each group (S1-S6) has their own set of latitudes/longitudes. The five low resolution channels have the same dimensions of *nscans* x 196 scan positions, while the high resolution channels have *nscans* x 392 scan positions. The high resolution geolocations from the A-scan (S5) are matched to each of the lower resolution channels (group S2-S4), then the B-scan (S6) are matched to the lower resolution channels. The retrieved data product therefore has 2x *nscan* x 392 scan positions. (Note later version of the Level 1C AMSR-E data from the NASA PPS will be processed with 243/486 scan positions).

The **AMSR2** data are grouped in a similar manner as that of AMSRE. However, the dimensions of the AMSR2 are greater with the lower resolution geolocations being *nscans* x 243 scan positions and the high resolution geolocations being *nscans* x 486, which with the A/B scans results in an output dimension of *nscans* x 486 scan positions.

Table 5: Geolocation groups for each sensor together with number of scan positions (Note (i) the *GMI uses the L1C-R product which provides co-aligned footprints across all channels and (ii) the NASA PPS AMSR-E and AMSR-2 data does not include the 6.7 GHz channels).*

SMMR	SSM/I	SSMIS	TMI	GMI	AMSR-E	AMSR-2
No groups 6.6 VH					(6.7 VH)	(6.7 VH)
No groups 10.7 VH			S1 10.65 VH	10.65 VH	S1 10.65 VH	S1 10.65 VH
No groups 18.7 VH	19.35 VH	S1 19.35 VH	19.35 VH	18.7 VH	S2 18.7 VH	S2 18.7 VH
No groups 21.0 VH	S1 22.235 V	22.235 V	S2 21.3 V	S1 23.8 V	S3 23.8 VH	S3 23.8 VH
No groups 37.0 VH	37.0 VH	S2 37.0 VH	37.0 VH	36.64 VH	S4 36.5 VH	S4 36.5 VH
	S2 85.5 VH	S3 91.66 VH	S3 85.5 VH	89.0 VH	S5 89.0 VHA	S5 89.0 VHA
					S6 89.0 VHB	S6 89.0 VHB
				165.5 VH		
				S2 183.31/3 V		
				183.31/7 V		
-	*nscans* x 64	*nscans* x 90	*nscans* x 104	*nscans* x 211	*nscans* x 196	*nscans* x 243
nscans x 94	*2x nscans* x 128	*nscans* x 180	*nscans* x 208	*nscans* x 211	*2x nscans* x 392	*2x nscans* x 486

4.4 Land/Ocean delineation

The retrieval of precipitation is generally different over land than over ocean and consequently retrieval schemes require knowledge of the land/ocean background before generating a retrieval. Some retrieval algorithms are valid only over the ocean while other algorithms have separate land/ocean components, thus it is necessary to determine whether a given sensor field of view is over ocean, land, or ocean/land mixed. To determine the surface type, the Terra Moderate Resolution Imaging Spectro-radiometer (MODIS) Land Water Mask MOD44W product (https://lpdaac.usgs.gov/products/mod44wv006/) was sourced. This data set identifies water on the Earth's surface at a resolution of 250m. This was processed to provide a global mask with a 0.05° sampling resolution, producing a global mask of 7200x3600 pixels of the percentage water: a value of 0 indicating no water, and a value of 100 indicating all water. The percentage water was calculated over a 50 x 50 km area across the globe to ensure equal-area treatment of the surface type. The selection of the surface type for the retrieval is reflected in the geophysical flag where bit #0 is set for land, and bit #1 is set for ocean.

4.5 Brightness Temperature Screening

All brightness temperatures required for a given rain algorithm are screened to ensure they all within a valid range of between 50 K to 350 K. In addition to this screening any available quality flags within the Level 1C data are also used: all of the NASA PPS Level 1C data have a quality flag for each group (S1, S2, S3, etc.) and if the relevant quality flag is bad, then a retrieval is not generated. If the data fails this screening the retrieval value is set to missing (-9999.9) and the algorithm flag bit #0 is set, together with the processing flag bit #1.

4.6 Sea-ice and Snow screening

All retrievals are screened for the presence of sea-ice and snow cover. To ensure consistency across the entire period the sea-ice and snow cover data generated by the ECMWF Reanalysis V5 (ERA-5) was obtained from the Copernicus Climate Data Store (https://cds.climate.copernicus.eu/#!/home). The data used were daily, quarter degree gridded products from 1979-2020. The location of each observation was checked against the ERA-5 data and if sea-ice or snow cover was present then the retrieval is set to missing (-9999.9) and the appropriate algorithm flag bit #0 set (missing), and the processing flag bit #2 (sea-ice) and/or bit #3 (snow) are set. In addition, the geophysical flag bit #2 is set for sea-ice and/or bit #3 is set for snow. This sea-ice/snow screening is the last step for all of the algorithms. This assures that all valid rain retrievals are free of both sea-

ice and snow cover as defined by the ERA-5 product.

4.7 **Product output files**

For each Level 1C data file that has any valid observations an output NetCDF-4 file of instantaneous rain rates is generated. The geolocation and precipitation retrievals are stored to 2 decimal places which is deemed to be sufficiently accurate given the engineering limitations and the retrieval accuracies. All data within these files are internally compressed within NetCDF using a deflation level=1 (on a 1 to 9 scale, where 1 indicates the least amount of compression). Within each data set are global attributes, ancillary variables and a geophysical flag which are common to all the precipitation products. Each retrieval algorithm generates an estimate of precipitation along with a processing flag and algorithm flag, together with a quality scores (see below).

4.7.1 Global Attributes

The global attributes of each file includes the beginning and ending date and time information that is derived from the first and last scan of the input file. The orbit number from the input file name is copied into the output file name. The starting/ending latitude and direction, together with the Equator crossing longitude and date/time are all based on the spacecraft data which are included in the Level 1C input files (except for SMMR). The Equator crossing longitude is taken from satellite's ascending node. For the SMMR data, where satellite latitude/longitude data are missing, the geolocations from the central scan position are used to extract these data.

4.7.2 Array Dimensions

All of the precipitation retrievals share common array dimensions: the two dimensional arrays such as rain rate, latitude, longitude, etc. have common array dimensions, '*npixel'*, the number of scan positions per scan, and '*nscan'* the number of scans for a given orbit.

4.7.3 Ancillary Variables

In addition to the precipitation retrievals a number of ancillary variables are included that are applicable across algorithms. These include latitude and longitude that comes from the Level 1C high-resolution channel geolocations, although truncated to 2 decimal places. In addition to the date/time variables (also from the Level 1 data), a character variable *scan_datetime* having the year, month, day, hour, minutes, seconds and hundredths of seconds in the format YYYY-MM-DDThh:mm:ss.ssZ is derived from the six input date/time variables. A common geophysical flag (byte variable) indicates whether a retrieval is over land (bit #0) or ocean (bit #1) (based on the MODIS derived land/ocean data), and over sea-ice (bit #2) abnd/or snow (bit #3) (based on the daily ERA-5 sea-ice and snow cover data).

4.7.4 Precipitation data and associated flags

The precipitation retrievals for each algorithm is stored in respective groups within each orbital file and composed of four variables: preipitation rate, processing flag, algorithm flag, and quality score.

4.7.4.1 Precipitation data

The precipitation is expressed in units of mm/hr and is truncated to two decimal places. A value of -9999.9 is set for missing/no-retrieval. No limits on the range of the values of the retrieved precipitation are imposed, although some techniques have intrinsic limits with the individual retrieval scheme.

4.7.4.2 Processing flag

The processing flag (byte) reflects any issues in retrieving the precipitation for that specific algorithm. A processing flag of zero indicates that there are no issues in processing the data. If any of the bits are set a missing value is assigned to the retrieval and bit #0 of the algorithm flag is set ('missing/no-retrieval'). Table 6 below summarizes the meaning of each bit.

Table 6: Processing flag bits.

bit #0	Set if latitude/longitude out of range
bit #1	Set if brightness temperature out of range
bit #2	Set if ERA-5 defined surface sea-ice
bit #3	Set if ERA-5 defined surface snow cover
bit #4-7	Unused

4.7.4.3 Algorithm flag

An algorithm flag is provided for each of the retrieved values of each algorithm. These flags are algorithm and footprint dependent and relate to either external issues (bad geolocation/Tbs: bit #0) or internal algorithm checks or information (bits #1-5). Table 7 below summarizes the meaning of each set bit, while Table 8 indicates which retrieval scheme checks for each criteria.

Table 7: Algorithm flag bits (see also Table 8)

bit #0	Set if not applicable or the retrieved value is missing
bit #1	Set if retrieved value is a replication of a low resolution at a high resolution footprint
bit #2	Set if algorithm determines surface to be sea ice
bit #3	Set if algorithm determines surface to be snow
bit #4	Set if algorithm determines surface to be desert
bit #5	Set if algorithm determines other surface screening
bit #6-7	Unused

Table 8: Flags as determined by the individual algorithm: note not all retrieval schemes check for surface conditions.

Algorithm	Not applicable (bit #0)	Replication (bit #1)	Sea-ice (bit #2)	Snow (bit #3)	Desert (bit #4)	Other (bit #5)*
AD1	X		X		X	
BA0	X					
BA1	X					
BA3	X					
FE1	X		X	X	X	
FE2	X	X	X			
FE3	X	X	X			
FE4	X		X	X	X	
FR1	X		X	X	X	
FR2	X		X	X	X	
IO1	X	X				
NR1	X				X	X
NR2	X	X			X	X
PR1	X					
SC2	X	X				

* See algorithm description

4.7.4.4 Quality Score

Each precipitation retrieval has a quality score (unsigned byte) which is a measure of the 'quality' or 'confidence'. As such this is a consistently applied qualitative measure based upon a quantitative comparison of the precipitation retrievals against precipitation data derived from the ERA-5 reanalysis. While the ERA-5 data may not be an ideal reference data set, it is a widely accepted data set and provides consistent data across the whole period of the precipitation record being compared here.

The processing steps for the calculation of the quality score are:
i) Monthly 0.25x0.25 degree ERA-5 precipitation data is averaged to 1x1 degree monthly data;

ii) Instantaneous precipitation retrievals for each of the products from the above algorithms is mapped and aggregated to 1x1 degree monthly;

iii) For each algorithm product, for each sensor and for each month of that sensor's record statistics are generated for the satellite product versus the ERA-5 product. For every 1x1 degree grid box, the surrounding 15-degree region is used to calculate the statistics, with a minimum number of 1000 samples to ensure a representative set of data from which to calculate the statistics.

iv) the correlation and bias/ratio statistics are then used, via a 2-dimensional look-up table, to assign a quality score ranging from 0 to 250 where zero is of the highest quality (and represents perfect correlation and bias/ratio), while 250 is the poorest quality (with low correlation and low/high bias/ration).

This quality score is applied consistently across the whole period of the data products generated, across all algorithms and across all sensors. Therefore, it is possible to assess the relative quality of each product for any retrieval generated, allowing users to select what they consider to be the 'best' product.

Bias-ratio

Correlation	0	0.1	0.2	0.3	0.4	0.5	0.6	0.7	0.8	0.9	1	1.1	1.2	1.3	1.4	1.5	1.6	1.7	1.8	1.9	2	2.1	2.2	2.3	2.4	2.5
0.975	250	250	250	233	150	100	67	43	26	13	7	12	21	31	41	50	60	70	80	90	100	110	120	130	140	150
0.925	250	250	250	234	151	102	70	48	33	24	21	23	29	37	45	54	64	73	83	92	102	112	122	132	142	151
0.875	250	250	250	236	154	106	75	56	43	37	35	37	41	46	53	61	70	78	87	97	106	116	125	135	144	154
0.825	250	250	250	239	158	112	83	65	55	51	49	50	53	58	64	70	78	86	94	103	112	121	130	139	148	158
0.775	250	250	250	242	163	119	92	77	68	65	64	64	67	70	75	81	87	95	102	110	119	127	136	145	154	163
0.725	250	250	250	246	169	127	102	89	82	79	78	78	80	83	87	92	98	105	112	119	127	135	143	151	160	169
0.675	250	250	250	250	176	136	114	101	95	93	92	92	94	97	100	105	110	116	122	129	136	143	151	159	167	176
0.625	250	250	250	250	184	146	125	114	109	107	106	107	108	110	113	117	122	127	133	139	146	153	160	168	176	184
0.575	250	250	250	250	192	156	137	128	123	121	120	121	122	124	127	130	134	139	144	150	156	163	170	177	185	192
0.525	250	250	250	250	201	167	150	141	137	135	134	135	136	138	140	143	147	151	156	162	167	174	180	187	194	201
0.475	250	250	250	250	211	179	163	155	151	149	148	149	150	151	154	157	160	164	169	174	179	185	191	197	204	211
0.425	250	250	250	250	221	191	176	168	165	163	163	163	164	165	167	170	173	177	181	186	191	196	202	208	215	221
0.375	250	250	250	250	232	203	189	182	179	177	177	177	178	179	181	184	187	190	194	198	203	208	214	219	225	232
0.325	250	250	250	250	243	216	202	196	193	191	191	191	192	193	195	197	200	203	207	211	216	220	225	231	237	243
0.275	250	250	250	250	250	228	216	209	207	205	205	205	206	207	209	211	214	217	220	224	228	233	238	243	248	250
0.225	250	250	250	250	250	241	229	223	221	219	219	219	220	221	223	225	227	230	233	237	241	245	250	250	250	250
0.175	250	250	250	250	250	254	243	237	235	234	233	234	234	235	237	239	241	244	247	250	250	250	250	250	250	250
0.125	250	250	250	250	250	250	250	250	249	248	247	248	248	249	250	250	250	250	250	250	250	250	250	250	250	250
0.075	250	250	250	250	250	250	250	250	250	250	250	250	250	250	250	250	250	250	250	250	250	250	250	250	250	250
0.025	250	250	250	250	250	250	250	250	250	250	250	250	250	250	250	250	250	250	250	250	250	250	250	250	250	250

Figure 2: Quality scores as a function of correlation and bias/ratio. A quality score of zero represents perfect correlation (=1.0) and bias/ratio (=1.0), while a value of 250 represents poor correlation and low/high bias/ratio.

5 ASSUMPTIONS AND LIMITATIONS

5.1 Data Delivery

Overall the P-FCDR represents an initial version of a long term, climate-scale, ensemble of satellite precipitation products with a measure of error and uncertainty. It attempts to provide the best available suite of products that can be used individually, as an ensemble, or as a benchmark against which, or alongside other precipitation products. As such, if the satellite observations provided by the NASA

PPS exist, a precipitation retrieval in this data set will exist.

5.2 Assumed performance

As with all data sets, a number of assumptions have been made at several stages throughout the generation of the precipitation dataset, be it at the algorithm selection level, processing level, or even in the generation of the errors and uncertainties. Where possible the assumptions made have been to reduce the errors within the dataset, both input data and the processed data. For example, the generation of the precipitation products of co-located footprints, which is often deemed unnecessary, was done in this data set to ensure consistency across all the different sensors. In addition, the adjustment of the brightness temperatures between the different sensor was necessary to ensure consistency between the sensors and through the data record.

6 REFERENCES

Adler, R.F., H-Y.M. Yeh, N. Prasad. W-K. Tao and J. Simpson, 1991: Microwave simulations of a tropical rainfall system with a three-dimensional cloud model. J. Appl. Meteor., 30, 924-953.

Adler, R.F., A.J. Negri, P.R. Keehn and I.M. Hakkarinen, 1993: Estimate of monthly rainfall over Japan and surrounding waters from a combination of low-orbit MW and geosynchronous IR data. J. Appl. Meteor., 32, 335-356

Adler, R.F., G.J. Huffman and P.R. Keehn, 1994: Global tropical rain estimates from microwave-adjusted geosynchronous IR data. Remote Sensing Review, 11, 125-152

Bauer, P. and P. Schlussel, 1993: Rainfall, total water, ice water, and water vapour over sea from polarized microwave simulations and Special Sensor Microwave/Imager data, j. Geophys. Res., 98, 20737-20759.

Ebert, E.E., M.J. Manton, P. Arkin, R.J. Allam, G.E. Holpin, and A. Gruber, 1996: Results of the GPCP Algorithm Intercomparison Programme, Bull. Am. Meteor. Soc. *77*, 12, 2875-2888. https://doi.org/10.1175/1520-0477(1996)077<2875:RFTGAI>2.0.CO;2

Ferraro, R.R., N.C. Grody and G.F. Marks, 1994: Effects of surface conditions on rain identification using the SSM/I. Remote Sensing Reviews. 11, 195-209.

Ferraro, R.R. and G.F. Marks, 1995: The development of SSM/I rain rate retrieval algorithms using ground based radar measurements. J. Atmos. Ocean. Tech., 12 755-770.

Ferriday, J.G. and S. K. Avery, 1994: Passive microwave remote sensing of rainfall with SSM/I: Algorithm development and implementation. J. Appl. Meteor., 33 1587-1596.

Fiore J.B. and N.C. Grody, 1990: A classification algorithms for monitoring snow cover and precipitation using SSM/I measurements. Fifth Conference on Satellite Meteorology and Oceanography, 3-7 September 1990, London, England. 237-240.

Grody, N.C. 1991: Classification of snow cover and precipitation using the Special Sensor Microwave/Imager (SSM/I). J. of Geophys. Res., 96, 7423-7435.

Haferman, J.L., E. N. Anagnostou, D. Tsintikidis, W. F. Krajewski, and T. F.Smith, 1996: Physically based satellite retrieval of precipitation using a 3D passive microwave radiative transfer model. J. Atmos.Oceanic Technol., 13, 832–850.

Hollinger, J., R. Lo, G. Poe, R. Savage and J. Pierce, 1987: Special Sensor Microwave/Imager Users Guide, Naval Research Laboratory, Washington D.C. 120pp.

Hollinger, J., 1989: DMSP Special Sensor Microwave/Imager Calibration/Validation Manual. Naval Research Laboratory, Washington D.C.

Hollinger, J.P., J.L. Peirce and G.A. Poe, 1990: SSM/I instrument evaluation. *IEEE Transactions on Geoscience and Remote Sensing* 28, 5, 781-790, doi: 10.1109/36.58964.

Hollinger, J.P. 1992: DMSP Special Sensor Microwave/Imager Calibration/Validation Manual Vol 2. Naval Research Laboratory, Washington D.C. 304pp.

Kidd, C., Kniveton, D. and Barrett, E.C., 1998: Advantage and disadvantages of statistical/empirical satellite estimation of rainfall. *Journal of Atmospheric Sciences* 55, 1576-1582.

Kidd, C., Huffman, G., Becker, A., Skofronick-Jackson, G., Kirschbaum, D., Joe, P. and Muller, C., 2017: So, how much of the Earth's surface is covered by rain gauges? *Bulletin of the American Meteorological Society*. 98, 69-78. DOI: http://dx.doi.org/10.1175/BAMS-D-14-00283.1

Kummerow, C.D., D.L. Randel, M. Kulie, N-Y. Wang, R. Ferraro, S. J. Munchak, and V. Petkovic, 2015: The Evolution of the Goddard PROFiling Algorithm to a Fully Parametric Scheme. *J. Atmos. Oceanic Technol.*, **32**, 2265–2280

Liu, G. and J.A. Curry, 1992: Retrieval of precipitation from satellite microwave measurement using both emission and scattering. J. Geophys. Res., 97, 9959-9974.

Skofronick-Jackson, G., Huffman, G., Petersen, W.A., Kirschbaum, D. and Kidd, C., 2017: The Global

Precipitation Measurement mission: Results after 2 years in orbit. *Accepted by the Bulletin of the American Meteorological Society.* http://dx.doi.org/10.1175/BAMS-D-15-00306.1

7 ACRONYMS

AMSR[E,-2]	Advanced Microwave Scanning Radiometer [Earth Observing System, -2]
ATBD	Algorithm Theoretical Basis Document
DISC	Data and Information Services Center
DMSP	Defense Meteorological Satellite Program
ECMWF	European Centre for Medium-range Weather Forecasting EUMETSAT European organization for the exploitation of Meteorological Satellites
FCDR	Fundamental Climate Data Record
GCOM-W	Global Change Observation Mission - Water
GMI	GPM Microwave Imager
GPM	Global Precipitation Measurement mission
GSFC	Goddard Space Flight Center
HDF	Hierarchical Data Format
LEO	low Earth orbit
NASA	National Aeronautics and Space Administration
NCEI	National Centers for Environmental Information (formerly NCDC)
NetCDF	Network Common Data Format
NOAA	National Oceanic and Atmospheric Administration
PMM	Precipitation Measurement Missions
PMW	Passive Microwave
PPS	Precipitation Processing System
SMMR	Scanning Multichannel Microwave Radiometer
SRDS	Surface Reference Data Set
SSM/I	Special Sensor Microwave/Imager (or SSMI)
SSMIS	Special Sensor Microwave Imager/Sounder
Tb	Brightness temperature
TMI	TRMM Microwave Imager
TRMM	Tropical Rainfall Measuring Mission

APPENDIX 1

List of archive short and long names for each data set.

Sensor	Satellite	Short name	Long name
SMMR	Nimbus-7	PRECIP_SMMR _NIMBUS7	NASA MEASURES Precipitation Ensemble based on SMMR Nimbus-7 NSIDC L1B Tbs
SSM/I	F08	PRECIP_SSMI_F08	NASA MEASURES Precipitation Ensemble based on SSM/I DMSP F08 NASA PPS L1C V06 Tbs
SSM/I	F10	PRECIP_SSMI_F10	NASA MEASURES Precipitation Ensemble based on SSM/I DMSP F10 NASA PPS L1C V06 Tbs
SSM/I	F11	PRECIP _SMI_F11	NASA MEASURES Precipitation Ensemble based on SSM/I DMSP F11 NASA PPS L1C V06 Tbs
SSM/I	F13	PRECIP_SSMI_F13	NASA MEASURES Precipitation Ensemble based on SSM/I DMSP F13 NASA PPS L1C V06 Tbs
SSM/I	F14	PRECIP_SSMI_F14	NASA MEASURES Precipitation Ensemble based on SSM/I DMSP F14 NASA PPS L1C V06 Tbs
SSM/I	F15	PRECIP_SSMI_F15	NASA MEASURES Precipitation Ensemble based on SSM/I DMSP F15 NASA PPS L1C V06 Tbs
SSMIS	F16	PRECIP_SSMIS_F16	NASA MEASURES Precipitation Ensemble based on SSMIS DMSP F16 NASA PPS L1C V05 Tbs
SSMIS	F17	PRECIP_SSMIS_F17	NASA MEASURES Precipitation Ensemble based on SSMIS DMSP F17 NASA PPS L1C V05 Tbs
SSMIS	F18	PRECIP_SSMIS_F18	NASA MEASURES Precipitation Ensemble based on SSMIS DMSP F18 NASA PPS L1C V05 Tbs
SSMIS	F19	PRECIP_SSMIS_F19	NASA MEASURES Precipitation Ensemble based on SSMIS DMSP F19 NASA PPS L1C V05 Tbs
TMI	TRMM	PRECIP_TMI_TRMM	NASA MEASURES Precipitation Ensemble based on TMI TRMM NASA PPS L1C V05 Tbs
GMI	GPM	PRECIP_GMI_GPM	NASA MEASURES Precipitation Ensemble based on GMI GPM NASA PPS L1C V05 Tbs
AMSRE	AQUA	PRECIP_AMSRE_AQUA	NASA MEASURES Precipitation Ensemble based on AMSRE AQUA NASA PPS L1C V05 Tbs
AMSR 2	GCOMW1	PRECIP_AMSR2_GCOMW1	NASA MEASURES Precipitation Ensemble based on AMSR2 GCOMW1 NASA PPS L1C V05 Tbs

APPENDIX 2

The project data represents a full record spanning 43 years (1978-2020) with a precipitation ensemble derived form 15 retrieval techniques across 15 sensors. The data is available from the NASA DISC with the following DOIs:

10.5067/MEASURES/NIMBUS7/SMMR/DATA201
10.5067/MEASURES/DMSPF08/SSMI/DATA201
10.5067/MEASURES/DMSPF10/SSMI/DATA201
10.5067/MEASURES/DMSPF11/SSMI/DATA201
10.5067/MEASURES/DMSPF13/SSMI/DATA201
10.5067/MEASURES/DMSPF14/SSMI/DATA201
10.5067/MEASURES/DMSPF15/SSMI/DATA201
10.5067/MEASURES/DMSPF16/SSMIS/DATA201
10.5067/MEASURES/DMSPF17/SSMIS/DATA201
10.5067/MEASURES/DMSPF18/SSMIS/DATA201
10.5067/MEASURES/DMSPF19/SSMIS/DATA201
10.5067/MEASURES/TRMM/TMI/DATA201
10.5067/MEASURES/GPM/GMI/DATA201
10.5067/MEASURES/AQUA/AMSRE/DATA201
10.5067/MEASURES/GCOMW1/AMSR2/DATA201

The format, metadata and documentation has been developed in co-ordination with the NASA DISC guidelines.

APPENDIX 3

An example program to read in the precipitation products shown below. It should be noted that the number of algorithms applied across all sensors and all months/years is consistent, although the number of scan lines (nscans) and the number of scan positions vary depending upon the individual sensor (see Table 5 above).

```
!  program to read rain rate data from SMMR,SSM/I,SSMIS,TMI,GMI,AMSRE,AMSR2
!  read_ensemble.f90
!
   implicit none
   character*120 file_name
   character*120 full_name
   character*9 infile
   character*4 chyear
   integer grpid
   integer instat,ncid,nfiles
   integer nscan_id,np_id,numchar_id
   integer npixel,nscan,numchar
   integer ifile,iend,iostat,stat,i,j
   integer nalgs

   integer lat_id,lon_id
   integer year_id,month_id,day_id
   integer hour_id,minute_id,second_id
   integer scan_datetime_id
   integer geo_id
   integer rr_id,rrp_id,rra_id,rrq_id
   integer ia
   real, dimension(:,:), ALLOCATABLE  ::  latitude
   real, dimension(:,:), ALLOCATABLE  ::  longitude
   integer, dimension(:), ALLOCATABLE :: year
   integer, dimension(:), ALLOCATABLE :: month
   integer, dimension(:), ALLOCATABLE :: day
   integer, dimension(:), ALLOCATABLE :: hour
   integer, dimension(:), ALLOCATABLE :: minute
   integer, dimension(:), ALLOCATABLE :: second
   character, dimension(:,:), ALLOCATABLE :: scan_datetime
   integer*1, dimension(:,:), ALLOCATABLE :: geo_flag

   real, dimension(:,:), ALLOCATABLE  ::  rain_rate
   integer*1, dimension(:,:), ALLOCATABLE :: proc_flag
   integer*1, dimension(:,:), ALLOCATABLE :: alg_flag
   integer*1, dimension(:,:), ALLOCATABLE :: quality_score

   real, dimension(:,:,:), ALLOCATABLE  :: rr_all
   integer*1, dimension(:,:,:), ALLOCATABLE :: pf_all
   integer*1, dimension(:,:,:), ALLOCATABLE :: af_all
   integer*1, dimension(:,:,:), ALLOCATABLE :: qs_all

   character*3 algname(15)
   include 'netcdf.inc'

   chyear='1996'
!  algorithm names used to get group id numbers.  One group for each algorithm.
   algname(1)='AD1'
```

```
   algname(2)='BA0'
   algname(3)='BA1'
   algname(4)='BA3'
   algname(5)='FE1'
   algname(6)='FE2'    ! Applicable for SMMR
   algname(7)='FE3'    ! Applicable for SMMR
   algname(8)='FE4'
   algname(9)='FR1'
   algname(10)='FR2'
   algname(11)='IO1'   ! Applicable for SMMR
   algname(12)='NR1'
   algname(13)='NR2'   ! Applicable for SMMR
   algname(14)='PR1'
   algname(15)='SC2'   ! Applicable for SMMR

   nalgs=15   ! number of rain algorithms

! number of input files. normally set this to a number that will
! exceed number of possible files.
   nfiles=5
!  'files.txt' is a list of input file names.
   infile='files.txt'
   write(6,*)'infile ',infile
   open(unit=11,file=infile,form='formatted')

   do ifile=1,nfiles   !begin orbit loop
   read(11,*,iostat=iend) file_name

   if(iend .lt. 0) then
   exit
   else
   endif
  full_name='/data2/common/data_L2A_V01E/SSMI/f13/'//chyear//'/'//file_name

! open my netcdf file
   instat=NF_OPEN(full_name,NF_NOWRITE,ncid)

!  read the file dimensions
   instat=NF_INQ_DIMID(ncid,"nscan",nscan_id)
   instat=NF_INQ_DIMLEN(ncid,nscan_id,nscan)

   instat=NF_INQ_DIMID(ncid,"npixel",np_id)
   instat=NF_INQ_DIMLEN(ncid,np_id,npixel)

   instat=NF_INQ_DIMID(ncid,"numchar",numchar_id)
   instat=NF_INQ_DIMLEN(ncid,numchar_id,numchar)

   write(6,*)'nscan = ',nscan
   write(6,*)'npixel = ',npixel
   write(6,*)'numchar = ',numchar

!! do array allocations and read the data
   ALLOCATE (latitude(npixel,nscan))
   ALLOCATE (longitude(npixel,nscan))

   ALLOCATE (year(nscan))
   ALLOCATE (month(nscan))
   ALLOCATE (day(nscan))
```

```
   ALLOCATE (hour(nscan))
   ALLOCATE (minute(nscan))
   ALLOCATE (second(nscan))
   ALLOCATE (scan_datetime(numchar,nscan))

   ALLOCATE (geo_flag(npixel,nscan))

   ALLOCATE (rain_rate(npixel,nscan))
   ALLOCATE (proc_flag(npixel,nscan))
   ALLOCATE (alg_flag(npixel,nscan))
   ALLOCATE (quality_score(npixel,nscan))

   ALLOCATE (rr_all(npixel,nscan,nalgs))
   ALLOCATE (pf_all(npixel,nscan,nalgs))
   ALLOCATE (af_all(npixel,nscan,nalgs))
   ALLOCATE (qs_all(npixel,nscan,nalgs))


!  Read the geolocations or latitudes and longitudes
   instat=NF_INQ_VARID(ncid,"latitude",lat_id)
   instat=NF_GET_VAR_REAL(ncid,lat_id,latitude)

   instat=NF_INQ_VARID(ncid,"longitude",lon_id)
   instat=NF_GET_VAR_REAL(ncid,lon_id,longitude)

! read all of the date/time variables: year, month, day, hour, minute,
! and second
   instat=NF_INQ_VARID(ncid,"year",year_id)
   instat=NF_GET_VAR_INT(ncid,year_id,year)

   instat=NF_INQ_VARID(ncid,"month",month_id)
   instat=NF_GET_VAR_INT(ncid,month_id,month)

   instat=NF_INQ_VARID(ncid,"dayofmonth",day_id)
   instat=NF_GET_VAR_INT(ncid,day_id,day)

   instat=NF_INQ_VARID(ncid,"hour",hour_id)
   instat=NF_GET_VAR_INT(ncid,hour_id,hour)

   instat=NF_INQ_VARID(ncid,"minute",minute_id)
   instat=NF_GET_VAR_INT(ncid,minute_id,minute)

   instat=NF_INQ_VARID(ncid,"second",second_id)
   instat=NF_GET_VAR_INT(ncid,second_id,second)

   instat=NF_INQ_VARID(ncid,"scan_datetime",scan_datetime_id)
   instat=NF_GET_VAR_TEXT(ncid,scan_datetime_id,scan_datetime)

   write(6,*)'sample scan_datetime ',(scan_datetime(i,1),i=1,23)

!  Get values for the geophyscial flag.
!  Bit 0 - land
!  Bit 1 - ocean
!  Bit 2 - ERA-5 Sea-ice
!  Bit 3 - ERA-5 Snow

   instat=NF_INQ_VARID(ncid,"geophysical_flag",geo_id)
   instat=NF_GET_VAR_INT1(ncid,geo_id,geo_flag)
```

```
!-----------------------------------------------------------------------
   do ia=1,nalgs     ! begin algorithm loop

   instat=NF_INQ_NCID(ncid,algname(ia),grpid)

!  Rain Rate
!  Rain rates are in units mm/hr and -9999.9 is the fill value
   instat=NF_INQ_VARID(grpid,algname(ia)//'_rain_rate',rr_id)
   instat=NF_GET_VAR_REAL(grpid,rr_id,rain_rate)
!  write(6,*)'grpid,rr_id ',grpid,rr_id

!  Processing Flag
!  The meanings of the bits for the processing flag are:
!  bit 0 - input lat/lons out of range
!  bit 1 - input brightness temperature out of range (<50 K or >350 K)
!  bit 2 - ERA-5 Sea-ice
!  bit 3 - ERA-5 Snow
   instat=NF_INQ_VARID(grpid,algname(ia)//'_processing_flag',rrp_id)
   instat=NF_GET_VAR_INT1(grpid,rrp_id,proc_flag)
!  write(6,*)'grpid,rrp_id ',grpid,rrp_id

!  Algorithm Flag
!  The meanings of the bits for the algorithm flag are:
!  bit 0 - algorithm retrieval not applicable (retrieval missing)
!  bit 1 - replication of low-resolution retrieval
!  bit 2 - Algorithm Sea-ice
!  bit 3 - Algorithm Snow
!  bit 4 - Algorithm desert, sand, or semi-arid
!  bit 5 - Algorithm other flag (bad input brigntess temperature data)
!          From Hughes negative polarization test.  Used only for
!          NR1 and NR2 only.

   instat=NF_INQ_VARID(grpid,algname(ia)//'_algorithm_flag',rra_id)
   instat=NF_GET_VAR_INT1(grpid,rra_id,alg_flag)
!  write(6,*)'grpid,rra_id ',grpid,rra_id

! Quality scores are a measure of retrieval quality based on correlation and
! and bias-ratio vs. ERA-5 reanalysis rain data.  Quality scores were saved
! as unsigned bytes.  Values of -1 (255 unsigned byte), indicate a missing
! quality score.
   instat=NF_INQ_VARID(grpid,algname(ia)//'_quality_score',rrq_id)
   instat=NF_GET_VAR_INT1(grpid,rrq_id,quality_score)
!  write(6,*)'grpid,rrq_id ',grpid,rrq_id

!  aggregate data into 3D arrays
      do i=1,nscan
      do j=i,npixel
       rr_all(j,i,ia)=rain_rate(j,i)
       pf_all(j,i,ia)=proc_flag(j,i)
       af_all(j,i,ia)=alg_flag(j,i)
       qs_all(j,i,ia)=quality_score(j,i)
      enddo
      enddo

   enddo    ! end of algorithm loop
   if(allocated(latitude))deallocate(latitude,stat=instat)
   if(allocated(longitude))deallocate(longitude,stat=instat)
```

```
if(allocated(year))deallocate(year,stat=instat)
if(allocated(month))deallocate(month,stat=instat)
if(allocated(day))deallocate(day,stat=instat)
if(allocated(hour))deallocate(hour,stat=instat)
if(allocated(minute))deallocate(minute,stat=instat)
if(allocated(second))deallocate(second,stat=instat)
if(allocated(scan_datetime))deallocate(scan_datetime,stat=instat)

if(allocated(geo_flag))deallocate(geo_flag,stat=instat)

if(allocated(rain_rate))deallocate(rain_rate,stat=instat)
if(allocated(proc_flag))deallocate(proc_flag,stat=instat)
if(allocated(alg_flag))deallocate(alg_flag,stat=instat)
if(allocated(quality_score))deallocate(quality_score,stat=instat)

if(allocated(rr_all))deallocate(rr_all,stat=instat)
if(allocated(pf_all))deallocate(pf_all,stat=instat)
if(allocated(af_all))deallocate(af_all,stat=instat)
if(allocated(qs_all))deallocate(qs_all,stat=instat)

instat=NF_CLOSE(ncid)
enddo  ! end of orbit loop
close(11)

stop
end
```